Collisional radiative models in plasmas

Beitr. Plasmaphys. 24 (1984) 5, 447—473

Collisional Radiative Models in Plasmas

B. VAN DER SIJDE, J. J. A. M. VAN DER MULLEN and D. C. SCHRAM
Physics Department, Eindhoven University of Technology, Eindhoven, The Netherlands.

Abstract

A review on collisional-radiative models in plasmas is given. Work of FUJIMOTO, BIBERMAN et al, DRAWIN and SEATON has been an important guide to compose this review. Ionizing, recombining and equilibrium plasmas are dealt with. Attention has been paid to the classification of CR models in phases, such as Corona phase, excitation saturation phase (ESP), Capture radiative cascade (CRC) phase and partial local thermal equilibrium (PLTE). A numerical model applied to the argon neutral system and an analytical model applied to the ESP and PLTE for ionizing plasmas are treated in more detail.

1. Introduction

In plasma physics, the distribution functions of atoms and ions over their excited states are studied in the framework of collisional-radiative models (CR models). In these models, the densities of the various excited states of a specific atom or ion are expressed as functions of a number of relevant parameters, such as the ground state density n_0 and the ion density n_i, the electron temperature T_e and -density n_e. The name of the models indicates that the densities of the excited states are determined by collisional and radiative processes and that transport phenomena can be neglected for these species (see section 2).

The study of CR models may have one or more of the following aims:

1) The determination of the distribution function of the excited states as a function of the parameters n_0, n_i, n_e, T_e, already mentioned but also of the transition probabilities A and escape factors Λ for spontaneous emission and rate coefficients C for collisional excitation.
2) The study of elementary processes such as collisional excitation and de-excitation, ionization and recombination, and of radiative processes, by comparing the model results with experimental data.
3) Diagnostic aims such as the determination of the n_0 or T_e-value from the measurement of the intensities of spectral lines. These intensites are a good measure for the densities of excited states. Such a determination requires a good knowledge of CR models, since excited state densities are dependent on a great number of parameters.
4) Model studies of discharges, light sources such as gaslasers and impurity concentrations in high temperature plasmas. Particularly for light sources, a CR model is essential for a reliable computation of the light production as a function of various parameters.

The field of CR models has been developed by e.g. BATES, KINGSTON, MCWHIRTER and HEARN [1, 2], GRIEM [3], DRAWIN et al [4, 5], BIBERMAN et al [6, 7], FUJIMOTO et al [8—10] and SEATON [34]. With the references cited in those papers, a great deal of the work on CR models is covered. These contributions have been focussed for the greater part on hydrogen and hydrogenlike ion systems, since in that case theoretical or semi-empirical formulae for collisional transitions from e.g. DRAWIN [5], JOHNSON [11], VRIENS and SMEETS [12] or VAN DE REE [27] are available. The expressions can be compared with experimental results to check the reliability of the model proposed. But also more complex systems as He [13], Ar [14] and Ar^+ [15] and several others have been studied, and are of great practical interest. A great difficulty in these cases is that there are hardly available cross-sections specific to these elements. Contributions specific to multiple ionized particles are from JACOBS and DAVIS [28] and to recombining systems from FURUKANE et al [29] and SEATON [34].

This contribution can be considered as a general review on Collisional-Radiative Models, mainly based on work of FUJIMOTO, BIBERMAN et al., DRAWIN, SEATON and our own group.

2. Limitations in the Applicability of the CR Models Described

We limit ourselves in this paper on several points:

1) We exclude from the description the presence of molecular species, such as molecular ions, and the processes, responsible for their creation and destruction such as associative ionization and dissociative recombination. These species are present ($\geqq 10\%$) in gaseous discharge conditions with very low ionization degrees $\alpha \leqq 10^{-6}$ and atom densities $n_0 \geqq 10^{23}$ m^{-3} [7b, 30]. The inclusion of molecular species into a CR model should require important changes in the design of these models, since e.g. vibrational and rotational states may be important.

2) We assume a Maxwellian velocity distribution for the electrons. The heavy particle temperatures T_i and T_a may be different from T_e. Three types of processes compete with each other with respect to the Maxwellization of the electrons: 1) elastic collisions between electrons, resulting in a Maxwellization time $\tau_M \sim n_e^{-2}$; 2) the energy loss due to inelastic collisions like excitation and ionization in a time $\tau_{in} \sim n_e^{-1} \cdot n_0^{-1}$ at ionization degrees for which excitations and ionization in the neutral atomic system are dominant; 3) elastic collisions between electrons and atoms resulting in a Druyvesteyn distribution in a time $\tau_D \sim n_e^{-1} n_0^{-1}$.

   In Ref [7b] and [31] it is estimated that usually the condition for a Maxwell distribution is fulfilled for $\alpha \geqq 10^{-4} - 10^{-6}$, so that a great class of strongly, medium, and weakly ionized plasmas are covered and only typical gaseous discharges do not satisfy this condition. Special cases with rapid electrons, e.g. from plasma-wall sheaths, require a specific description, since only a small amount of them may dominate the excitation and ionization processes.

3) We limit ourselves to electron (e) excitations and ionization processes and exclude from the description heavy particles (a) collisions leading to excitation and ionization. These processes can also be neglected for large enough ionization degrees. For the same temperatures, the excitation and ionization rates for heavy particles are about a factor 10^3 smaller, since the velocity $v_a \approx 10^{-2} v_e$ and the cross-sections are assumed to be a factor 10 smaller than for electronic collisions. This leads to a dominance for e-a inelastic processes for $\alpha \geqq 10^{-3}$. In Ref [7b] several references on this topic can be found.

A special case in this respect is charge exchange in two or multispecies plasmas. This process has large cross-sections and is in many cases responsible for excitation, ionization transfer from one to another component of the plasma [32].

By the limitations outlined above we treat CR models with electronic (de)-excitation, ionization and recombination processes and with radiative processes as spontaneous emission, absorption and, possibly stimulated emission.

3. The Basic Set-up of CR Models

The basic set-up of numerical CR models is the formation of a number of coupled differential equations for the densities of excited states:

$$\frac{\partial n(p)}{\partial t} + \nabla.(n(p)\,\boldsymbol{w}_p) = \left(\frac{\partial n(p)}{\partial t}\right)_{c,r} \tag{1}$$

The same type of equation holds for n_0 and n_i. The changes from collisional (c) and radiative (r) processes are taken into account in the term at the right hand side. The first term is the time derivative and the second term is the transport term by diffusion and convection.

A typical situation for excited states is that the contribution of populating and depopulating c.r. processes separately is very large with respect to the $\partial n(p)/\partial t$ and $\nabla.(n(p)\mathrm{w}_p)$ term. Therefore, the basic set-up mentioned, is simplified in the so-called quasi-steady-state-solution (QSSS) by assuming that

$$\frac{\partial n(p)}{\partial t} = 0; \quad \nabla.(n(p)\,\boldsymbol{w}_p) = 0 \tag{2}$$

for excited states. Then the eqs. (1) can be replaced by a number of coupled linear equations [2]:

$$\left(\frac{\partial n(p)}{\partial t}\right)_{c,r} = 0. \tag{3}$$

For the ground state 0 and the ion ground state i, the full eq. (1) applies. For these states, the gain and loss parts of the c, r term are in many cases not of the same magnitude. This results in a significant transport term and/or a rate of change of the ground state densities. In fact, we consider the eqs. (1), (3) in separate time domains, a long time domain for ground states and a short time domain for excited states (multiple time scale). In the short time domain, there is no relevant time dependent behaviour and no relevant transport for excited states, whereas for the long time domain the densities $n(p)$ are dependent on the slowly varying n_0 and n_i. Since the coupling from the ground states to the excited states is slow, but that from excited states to other excited states and from excited states to ground states is much more rapid, the description is correct [2]. For low n_e-values, the assumption of QSSS can be violated by metastables, since the rapid time behaviour of spontaneous emission lacks in this case.

The set of linear equations for $p = 1$ to N can be solved numerically in terms of the densities n_0 and n_i. One can either solve these ground state densities with the aid of eq. (1), including the transport and time dependent terms, or one can introduce them as independent input parameters. To be sure in that case whether a physically consistent set of parameters is chosen, one has to measure these parameters.

For analytical models, the QSSS can also be followed. In this case one tries to set up one general equation, valid for every excited state, by assuming (de)excitation rates and radiative processes which are analytical functions of e.g. the excitation energy or, which is equivalent, the principal quantum number $(pqn)p$. It is clear that significant deviations from a mean, predictable behaviour falls out of the scope of analytical models so that e.g. inversion of state densities cannot be found for ionizing plasmas.

As a consequence of the QSSS, it is convenient to describe a density $n(p)$ as a function of the ground state densities n_0 and n_i according to

$$n(p) = r^0(p)\, Q^S(p) \cdot n_i + r^1(p) \cdot Q^B(p) \cdot n_0. \tag{4}$$

This can also be written as

$$n(p) = r^0(p) \cdot n^S(p) + r^1(p) \cdot n^B(p) \tag{5}$$

in which $n^S(p)$ and $n^B(p)$ are the Saha density and Boltzmann density, respectively The so-called collisional-radiative coefficients $r^0(p)$ and $r^1(p)$ give the deviations with respect to $n^S(p)$ and $n^B(p)$; $Q^S(p)$ and $Q^B(p)$ are factors containing a part of the Saha equation and the Boltzmann equation according to

$$Q^S(p) = n_e \cdot g_e^{-1} \cdot g_i^{-1} \cdot g(p) \cdot (h^2/2\,\pi m_e kT_e)^{3/2} \exp\,(E_{ip}/kT_e), \tag{6a}$$

and

$$Q^B(p) = g(p) g_0^{-1} \exp -(E_{ep}/kT_e), \tag{6b}$$

with E_{ip} = the ionization energy for p and E_{ep} = the excitation energy for p; $g_e = 2$ is the statistical weight for electrons, g_i for ions and g_0 for the ground state and $g(p)$ for p. The first term of eq. (5) indicates the density $n(p)$ in the case that $n_0 = 0$ and the second terms indicates that density for $n_i = 0$. It is convenient to describe the behaviour of CR models in terms of $r^0(p)$ and $r^1(p)$. These coefficients are functions of n_e and T_e, but also of the escape factors $\Lambda(p)$, which in their turn are dependent on the plasmadimensions R_p, the heavy particle temperature T_a or T_i and of the ground state density itself. For large $k_0 R_p$ values it is important that Stark broadening is taken into account. Then also the electron density n_e influences the value of Λ; $k_0 R_p$ is the so-called optical depth.

4. Mainlines of the Description of CR Models

4.1.0. Classification according to plasma state

For a proper understanding of the interpretation of CR models, it is very important to distinguish between 3 kinds of plasmas:

1. Ionizing plasmas;
2. Recombining plasmas;
3. Equilibrium plasmas.

This classification is based on the fact whether a plasma is in ionization-recombination equilibrum or not. The term equilibrium plasmas in this context does not mean plasmas in some kind of thermal equilibrium, but merely the absence of a nett ionization or recombination. It may be clear that for ionizing and recombining plasmas, there is such a nett activity.

4.1.1. Ionizing plasmas

Ionizing plasmas are characterized by an ionization term $S_{CR} n_e n_0$ and a recombination term $\alpha_{CR} n_e n_i$ which are related to each other according to

$$S_{CR} n_e n_0 - \alpha_{CR} n_e n_i > 0 \tag{7}$$

S_{CR} is the ionization rate coefficient and α_{CR} the recombination rate coefficient, as defined by BATES et al [1].

Ionizing plasmas may in a steady state, with $\partial n_0/\partial t = \partial n_i/\partial t = 0$. In that case, inward transport of ground state atoms and outward transport of ion ground state particles are needed to compensate for the net ionization activity.

Ionizing plasmas may be also time dependent, $\partial/\partial t \neq 0$, with or without diffusion of ground state particles. The density n_0 is given by

$$\partial n_0/\partial t = - S_{CR} n_e n_0 + \alpha_{CR} n_e n_i - \nabla \cdot (n_0 \boldsymbol{w}_0) \tag{8}$$

and the density n_i by

$$\partial n_i/\partial t = + S_{CR} n_e n_0 - \alpha_{CR} n_e n_i - \nabla \cdot (n_i \boldsymbol{w}_i) \tag{9}$$

The main processes for the plasmas are shown in Fig. 1.

Examples of ionizing plasmas are several types of current carrying discharges such as arcs, positive columns, gas lasers, active parts of flames and so on.

4.1.2. Recombining plasmas

Recombining plasmas are characterized by the relation

$$S_{CR} n_e n_0 - \alpha_{CR} n_e n_i < 0 \tag{10}$$

Recombining plasmas may also be in a steady state, $\partial/\partial t = 0$, but now with inward transport of ions and outward transport of ground state atoms, just reverse to ionizing plasmas. The same time-dependent equations (8, 9) as for ionizing plasma are valid. The main processes for these plasmas can be found in Fig. 2.

Examples of recombining plasmas are many types of non-current carrying plasmas such as after-glows, the non-active part of plasma torches, outer regions of flames and so on.

4.1.3. Equilibrium plasmas

Equilibrium plasmas are formally characterized by the relation

$$-\partial n_0/\partial t - \nabla \cdot (n_0 \boldsymbol{w}_0) = \partial n_i/\partial t + \nabla \cdot (n_i \boldsymbol{w}_i) = S_{CR} n_e n_0 - \alpha_{CR} n_e n_i = 0. \tag{11a}$$

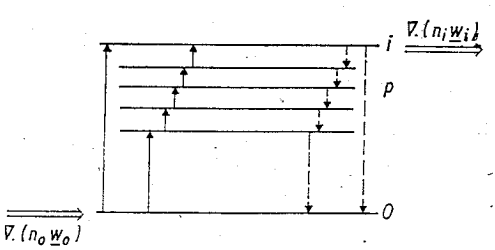

Fig. 1. The main stream of processes in an ionizing plasma

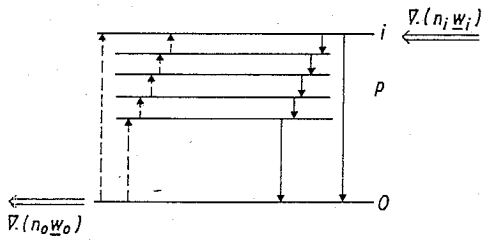

Fig. 2. The main stream of processes in a recombining plasma

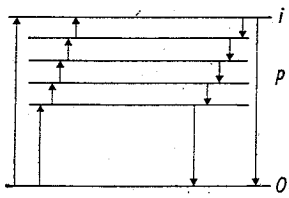

Fig. 3. The main stream of processes in an equilibrium plasma

In most cases one can state that

$$-\partial n_0/\partial t = \partial n_i/\partial t = S_{CR} n_e n_0 - \alpha_{CR} n_e n_i = 0 \qquad (11b)$$

is valid, it means that equilibrium plasmas are in a steady state, since there is no inward or outward transport of ground state atoms and ions.

The main processes are a combination of those in Fig. 1 and Fig. 2, but now without the $\nabla \cdot (n\mathrm{w})$ contributions. Examples of equilibrium plasmas are transitions zones between ionizing and recombining plasmas. The description is also important for near equilibrium plasmas.

4.2.0. Classification depending on the electron density n_e and the principal quantum number p

Besides a classification in the three types, mentioned above, we can discern a further classification in phases like corona phase, excitation saturation phase (ESP) and so on. Whether a plasma is in one or another phase depends mainly on the electron density n_e and less on the electron temperature T_e, the neutral density n_0 and the ion density n_i in cases where $n_i \neq n_e$. In fact, generally it is a simplification to say that a plasma is in one or another phase, since it is quite normal that for a specific ionizing plasma condition the lower states are in the corona phase, medium states are in ESP and higher states are in partial LTE (PLTE). Thus, the phase of a particular state p depends on n_e and other parameters and on the value of p itself. We shall describe in this section phase classification according to these remarks.

4.2.1. Ionizing Plasmas

4.2.1.1. Corona Phase

For sufficientyl low n_e-values, e.g. for a hydrogen plasma with $T_e \approx 3$ eV for $n_e \leqq 1.10^{20}$ m^{-3}, one or more states with sufficiently low p-values can be described with the corona phase (see Fig. 8). In its most elementary form, we can state that excited states

p are populated by direct excitation from the ground state and are depopulated by spontaneous emission of radiation to lower states. It means that there is no excitation flow to higher states and to the ion ground state from these lower excited states and that there is only direct ionization from the ground state to the ion state. Recombination does not play any role at these low n_e-values since recombination is proportional to $n_e^2 n_i$ (three body recombination) or $n_e n_i$ (radiative recombination) and is much smaller than outward ion transport. See also the Figs. 11—14 from which it is clear that $r^1(p) n^B(p) \gg r^0(p)\, n^S(p)$. Thus, only the second term of eq. (5), $r^1(p)\, n^B(p)$, contributes to $n(p)$; this is consistent with the ionizing character of the plasma.

In this most elementary form, the balance equation for an optically thin plasma can be written as

$$C(0, p) \cdot n_e \cdot n_0 = \sum_{q<p} A(p, q) \cdot n(p), \tag{12}$$

with C is an excitation rate coefficient. In some cases, cascade radiation from higher states has to be taken into account and in other cases stepwise excitation is introduced by metastable states.
Then, eq. (12) has to be extended to:

$$C(0, p) \cdot n_e \cdot n_0 + C(m, p) \cdot n_e \cdot n_m + \sum_{r>p} A(r, p) \cdot n(r) = \sum_{q<p} A(p, q) \cdot n(p), \tag{13}$$

with the index m for a metastable state. The $r^1(p)$ coefficients are $\ll 1$ and proportional to n_e for the corona phase. The latter can be found as a consequence of the structure of the populating and depopulating processes in the eqs. (12, 13).

Fujimoto [10] introduced a description to characterize the density per unit statistical weight $\eta(p) = n(p)/g(p)$ in terms of the $pqn\,p$. He deduced for the temperature range of ionizing plasmas

$$n(p)/g(p) \sim p^{-0.5} \tag{14}$$

for optically thin plasmas. Absorption of resonance radiation gives large deviations from this power law. The main processes for the corona phase are indicated in Fig. 4.

4.2.1.2. Excitation saturation Phase (ESP)

For a hydrogen plasma with $T_e \approx 3$ eV all excited states are in ESP for $ne \geqq 10^{21}\,\mathrm{m}^{-3}$, whereas for lower n_e-values a decreasing number of higher states is in this phase (Fig. 8). The dominant characteristic for this phase is that for these higher n_e and/or p-values the collisional excitation — radiative deexcitation balance of the corona phase is re-

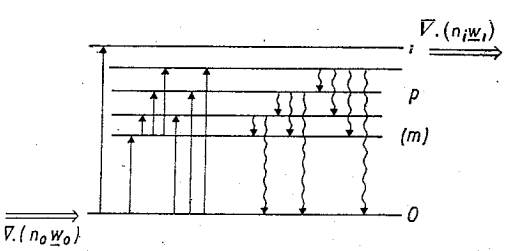

Fig. 4. The main processes in the corona phase of an ionizing plasma

placed by a collisional excitation — deexcitation balance; the ESP is thus collisionally dominated. The balance equation for a state p can then be written as:

$$n_e \cdot \sum_{q \neq p} C(q, p) \cdot n(q) + (n_e \cdot \alpha(p) \cdot n_i) = n_e \cdot \sum_{q \neq p} C(p, q) \cdot n(p) + n_e \cdot S(p) \times n(p), \qquad (15)$$

with $S(p)$ is the ionization rate coefficient. The recombination term $n_e \cdot \alpha(p) \cdot n_i$ is of minor significance here and has been indicated for completeness.
The specific character of these deexcitation processes is that they create a ladderlike excitation flow from lower to higher excited states, pre-dominantly with steps of $\Delta p = 1$ for hydrogen and $\Delta p \leqq 1$ for e.g. argon. Here p is the effective pqn. In addition there is from every state a certain chance of ionization to the ion ground state (see Fig. 5).

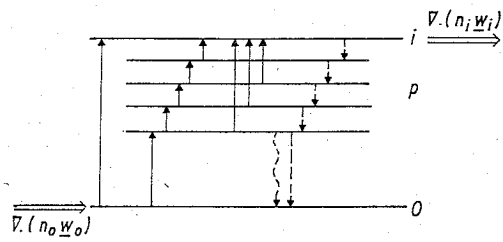

Fig. 5. The main processes in the excitation saturation phase of an ionizing plasma

Thus in spite of the fact that the plasma is collisionally dominated, there is no Saha-equilibrium between the excited states but, apart from an ionization sink at every state p, a balance between the excitation from state $p-1$ to p and the deexcitation from p to $p+1$. Excitation to upper states is favoured with respect to lower states by larger excitation cross-sections as a consequence of a smaller energy gap between the excited states and of an increasing statistical weight for higher excited states, e.g. $2p^2$ for hydrogen. The condition for ladderlike excitation is that $p >$ the Byron limit $p_{By} = (Ry/3\,kT_e)^{1/2}$. This condition is fulfilled for all excited states for ionizing plasmas if $T_e > 1.0$ eV. The deviations from Saha-equilibrium are due to the absence of a significant recombination contribution. It means that the term $r^0(p)\,n^S(p)$ of eq. (5) plays a minor role. The absence of a significant recombination is related to not too high electron densities and not too low ground state densities, $n_0/n_i \gg \alpha_{CR}/S_{CR}$ Eq. (15) can be replaced by

$$C(p-1, p) \cdot n_e \cdot n(p-1) - C(p, p-1) \cdot n_e \cdot n(p) = C(p, p+1) \cdot n_e \times n(p) - C(p+1, p) \cdot n_e \cdot n(p+1) + S(p) \cdot n_e \cdot n(p) - (\alpha(p) \cdot n_e \cdot n_i). \qquad (16)$$

The relative overpopulation with respect to the Saha density $\delta b(p) = n(p)/n^S(p) - 1$ is according to VAN DER MULLEN et al [16] (see section 6)

$$\delta b(p) = b_0 p^{-6}, \qquad (17a)$$

or with $\eta(p) = n(p)/g(p)$,

$$\eta(p) = \beta p^{-6} \exp E_{ip}/kT_e + \eta^S(p). \qquad (17b)$$

Since $\exp E_{ip}/kT_e \approx 1$ for $E_{ip}/kT_e \to 0$, the p^{-6} power law is the most important factor in cases with not too low temperatures.

An important part of the total ionization is in ESP for not too high temperatures governed by stepwise ionization. This is a consequence of the existence of the ladderlike excitation flow.

According to eq. (17) $r^1(p) \sim p^{-6}$, thus strongly dependent on p; the coefficient seems to be independent of n_e and is only weakly dependent on T_e. Typical values are 10^{-2} to 10^{-5}, thus $\ll 1$, for $p = 2$—6 for hydrogen (Fig. 10). The fact of $r^1(p)$ values, independent of n_e, is in agreement with the structure of the eqs. (15, 16), since all terms are in the same way dependent on n_e. In fact, there is for many excited states a smooth transition between the corona phase with $r^1(p) \sim n_e$ and a typical ESP with $r^1(p) =$ constant for a certain p-value. This comes from the fact that transition from radiative deexcitation in the corona phase to collisional deexcitation in the ESP takes place at different n_e-values for different excited states. Lower states come into ESP for higher n_e-values and deliver above that value their full contribution to the excitation flow. As a consequence, the density of higher states increases, in spite of the structure of the eqs. (15, 16) until the lowest excited state is in ESP. From that n_e-value the system is in so-called complete saturation, and all $r^1(p)$ values become constant, independent of n_e. Below that specific n_e-value the $r^1(p)$ behaviour is between that of corona and that of complete saturation (see also Fig. 9).

The construction of the eqs. (17a) and (17b) leads to a better understanding of the different density distributions over the excited states for sufficiently high T_e-values, say $T_e > 1.5$ eV in argon and hydrogen with respect to low T_e-values, say $T_e < 1.0$ eV. For high T_e-values $\eta(p)$ should follow a p^{-6} dependence and for low T_e- and p-values $\eta(p)$ should follow an $\exp(E_{ip}/kT_e)$ dependence.

We now can explain this behaviour as follows:
Since b_0 (and β) > 0 for ionizing plasmas, $\delta b(p) > \delta(p+1)$ in eq. (17a), which leads to a ladderlike excitation flow in upper direction; this conclusion is valid for high and low T_e-values, since the direction of the flow is determined by the value of $\delta b(p)$ with respect to $\delta b(p+1)$.

The density $\eta(p)$ itself or $\delta\eta(p) = \eta(p) - \eta^S(p)$ is determined by $\beta p^{-6} \exp(E_{ip}/kT_e)$ and not only by βp^{-6} as stated by Fujimoto. For high T_e-values, the slope of the p^{-6} factor is indeed dominant over that of the factor E_{ip}/kT_e. For low T_e-values, however, the p^{-6} factor is no longer dominant for low p-values. This role is taken over by the factor $\exp(E_{ip}/kT_e)$ (see Fig. 6) and leads to a close to Saha density. Without taking into account the factor $\exp(E_{ip}/kT_e$ in $\eta(p)$, one comes to the erroneous conclusion that for low T_e- and p-values $\delta b(p) < \delta b(p+1)$, though $\delta\eta(p) > \delta\eta(p+1)$. This should lead to an excitation flow into lower direction, a behaviour contrary to the ionizing character of the plasma. We conclude that this misinterpretation is avoided by the introduction of $\exp E_{ip}/kT_e$ in $\eta(p)$, since now $\delta b(p) = b_0 p^{-6}$ for all temperature and $\delta\eta(p)$ is dominated by either $\exp(E_{ip}/kT_e)$ or p^{-6}, leading to two different density distributions, described by one formula. For values $p < p_{By}$, the boundary value given by the Byron limit, the densities are dominated by the factor $\exp(E_{ip}/kT_e)$ and the states show a small deviation from thermal equilibrium, a near equilibrium situation. The excitation flow, which at first sight seems to be limited in this situation by the near equilibrium values of $\eta(p)$ and $\delta\eta(p)$, retains its magnitude, since the flow depends only on the difference between $\delta b(p)$ and $\delta b(p+1)$. Only the relative value of the flow is small with respect to the many equilibrium processes which take place. In section 6 (eqs. 30, 33a), this point becomes more clear.

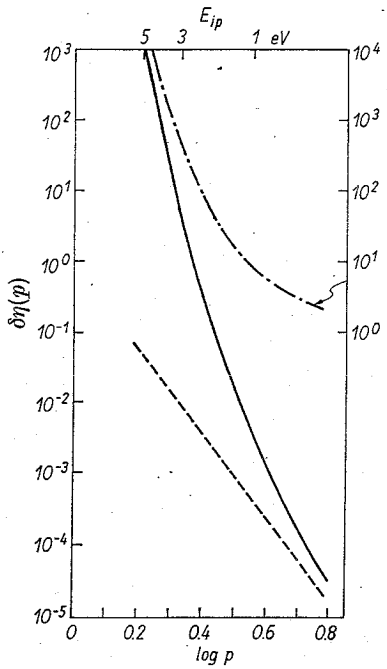

Fig. 6. The density
$\delta\eta(p) = \eta(p) - \eta^S(p) = \beta p^{-6} \exp E_{ip}/kT_e$
of excited states in an ionizing plasma
for $T_e = 0.5$ eV;
– – –: p^{-6};
– · –: $\exp E_{ip}/kT_e$;
——: $p^{-6} \cdot \exp E_{ip}/kT_e$

4.2.1.3. Partical Local Thermal Equilibrium (PLTE)

For an ionizing plasma three body recombination becomes important at high n_e-values. In fact, also here the influence of recombination is first demonstrated for high p-vales and becomes important for lower states with increasing n_e-values (see Fig. 25, the phase diagram for argon). When the total number of recombination processes to a certain state p is almost equal to that of ionization processes and largely exceeds the excitation flow, this state is in Saha-equilibrium or in PLTE. As a consequence of the Saha-equilibrium, there is also an excitation-deexcitation equilibrium between state p and its neighbouring states $p - 1$ and $p + 1$, apart from the excitation flow, which is now relatively small with respect to the large number of equilibrium processes. However, this flow retains its magnitude, and still determines the ion density, since the excitation flow determines for an important part the total ionization.

As a consequence of the dominance of ionization-recombination and excitation-deexcitation equilibrium, only the term $r^0(p)\, n^S(p)$ of eq. (5) is important and for p-values high enough, $r^0(p) = 1$. In PLTE, the coefficient $r^1(p)$ retains its value reached in ESP and is still $\ll 1$. The dominant processes in PLTE are shown in Fig. 7. In PLTE eq. (16) remains valid, the recombination term included.

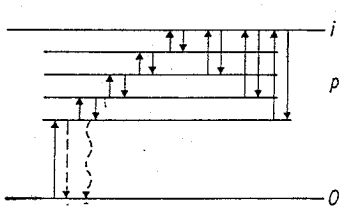

Fig. 7. The main processes in the partial LTE of an ionizing plasma

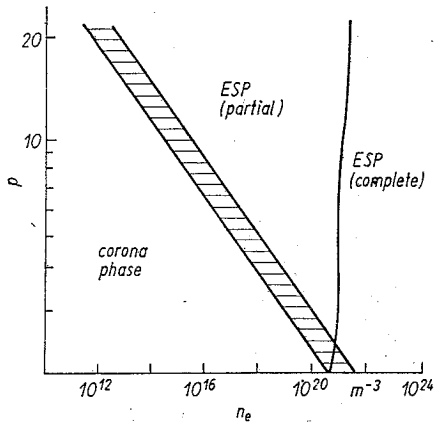

Fig. 8. Phase diagram for an optically thin ionizing hydrogen plasma at $T_e = 1.28 \times 10^5$ K, according to FUJIMOTO (10b)

An overall view of the phases as functions of p and n_e is given in Fig. 8 for hydrogen and in Fig. 25 for argon. In these figures the distinction between complete and partial saturation is also indicated. The boundary between ESP and PLTE depends on the n_0-value used (Fig. 25); this is a consequence of a larger excitation flow for larger n_0-values. The boundary criterion used is: $n(p)/n^S(p) = 2$. Since $n(p)$ is proportional to n_0 and $n^S(p)$ to $n_e \cdot n_i$, we find that for the boundary condition $n(p)/n^S(p) \sim n_0/n_e n_i$ ($= n_0/n_e^2$ for singly ionized plasmas) = constant. A change of a factor 100 in n_0 corresponds with a change of a factor 10 in n_e.

In the Figs. 9 and 10 we give examples of the $r^1(p)$ coefficients for hydrogen plasmas deduced from data of DRAWIN and EMARD [5b], one for an optically thin plasma (Fig. 9) and one for an optically thick plasma (Fig. 10). These Figs. demonstrate the behaviour of the $r^1(p)$ coefficients in the corona and ESP phase as described, e.g. the constant value for high n_e-values. Note the influence of radiation trapping. For the optically thick

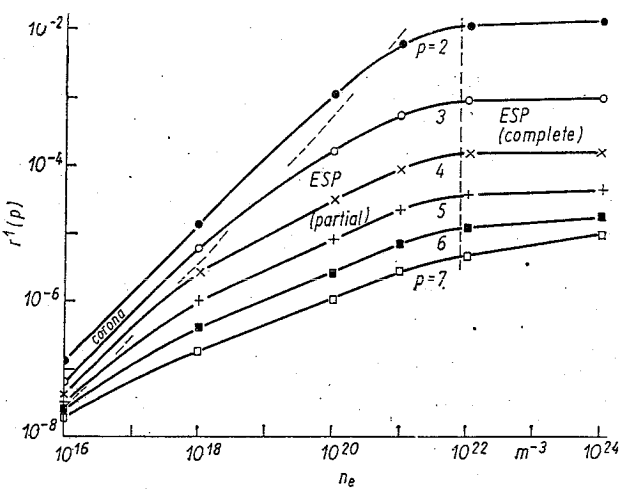

Fig. 9. The $r^1(p)$ coefficients for an optically thin hydrogen plasma (Ref. [5b]) as a function of the elctron density; $T_a = 32 \cdot 10^3$ K

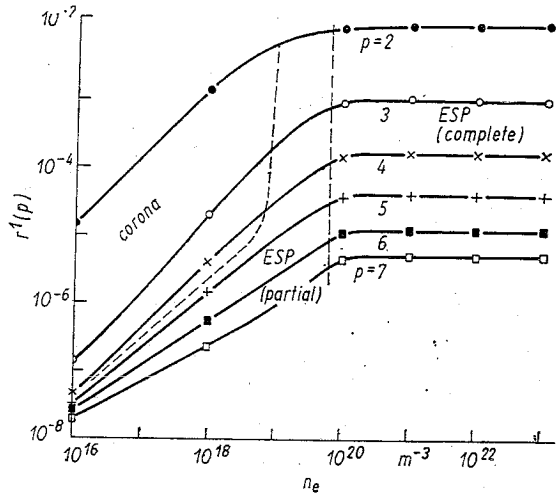

Fig. 10. The $r^1(p)$ coefficients for an optically thick hydrogen plasma (Ref. [5b]) as a function of the electron density n_e;
$T_e = 32 \cdot 10^3$ K; $\Lambda(2,1) = 10^{-2}$, $\Lambda(3,1) = 10^{-1}$.

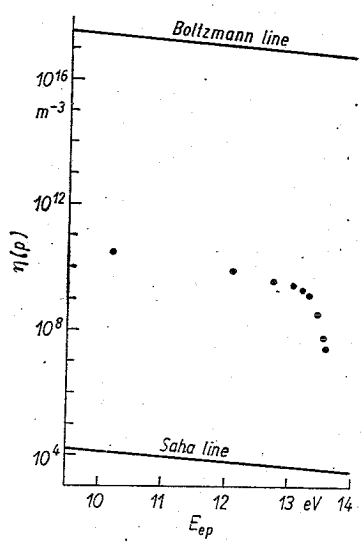

Fig. 11. The density of excited states per unit of statistical weight $\eta(p) = n(p)/g(p)$ as a function of the excitation energy E_{ep}, a so-called Boltzmann-plot for an optically thin hydrogen plasma. Parameters: $n_e = 10^{16}$ m^{-3}, $T_e = 32.000$ K, $n_0 = 10^{19}$ m^{-3}. The Boltzmann- and Saha-densities are also indicated as Boltzmann- and Saha-line, respectively.

case the $r^1(p)$ values are already constant at $n_e \geqq 10^{20}$ m^{-3} and for the optically thin case at $n_e \geqq 10^{22}$ m^{-3}. In the Figs. (11—14) we show for a hydrogen plasma with $T_e = 32 \cdot 10^3$K and $n_0 = 10^{19}$ m^{-3} the densities of excited states for a number of electron densities, from $n_e = 1 \cdot 10^{16}$ m^{-3} till $n_e = 1 \cdot 10^{22}$ m^{-3}. For $n_e = 1 \cdot 10^{16}$ m^{-3} and $1 \cdot 10^{18}$ m^{-3} these

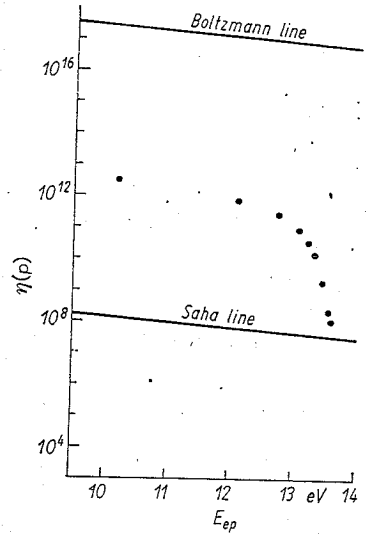

Fig. 12. The same Boltzmann-plot, for $n_e = 10^{18}$ m^{-3}, $T_e = 32.000$ K, $n_0 = 10^{19}$ m^{-3}

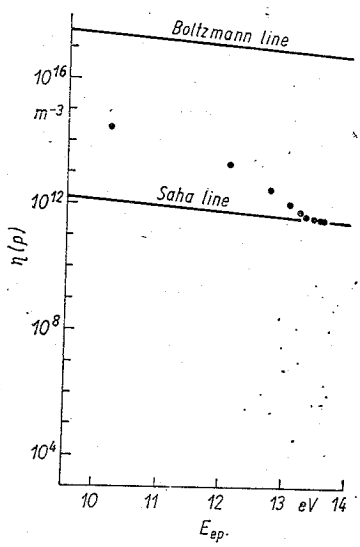

Fig. 13. A Boltzmann-plot for $n_e = 10^{20}$ m^{-3}, $T_e = 32.000$ K, $n_0 = 10^{19}$ m^{-3}

densities are all between the line of Boltzmann densities $n^B(p)$ and that of Saha densities $n^S(p)$. For $n_e = 1.10^{20}$ m^{-3}, $n(p) = n^S(p)$ for the highest states indicated, namely $p \geqq 10$ and for $n_e = 1.10^{22}$ m^{-3} almost all states are in PLTE. The Saha-line shifts towards the Boltzmann line, since $n^S(p) \sim n_e n_i = n_e^2$, so that full LTE is reached at about $n_e = 5.10^{22}$ m^{-3}.

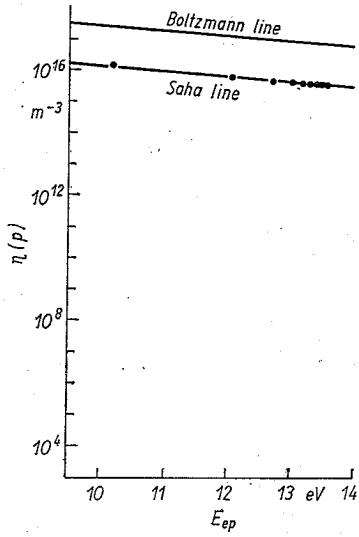

Fig. 14. A Boltzmann-plot for $n_e = 10^{22}$ m^{-3}, $T_e = 32.000$ K, $n_0 = 10^{19}$ m^{-3}

4.2.2. Recombining Plasmas

4.2.2.1. Capture Radiative Cascade (CRC) Phase

Recombining plasmas are for sufficiently low n_e- and p-values in the so-called CRC phase. In this phase the population density of a state p is completely determined by radiative processes; this is contrary to the corona phase, with both collisional and radiative processes. In its most elementary form, a state p is populated by radiative recombination and depopulated by spontaneous emission to lower states. The ionization and excitation energy is transfered into radiation by several steps of cascade radiation. In this case the balance equation for a state p reads:

$$n_e \cdot n_i \cdot \beta(p) = n(p) \sum_{q<p} A(p, q), \tag{18a}$$

where $\beta(p)$ is the coefficient for radiative recombination. If we take into account the contribution of cascade radiation from higher states than p itself, eq. (18a) has to be extended to

$$n_e \cdot n_i \cdot \beta(p) + \sum_{r>p} n(r) \cdot A(r, p) = n(p) \cdot \sum_{q<p} A(p, q). \tag{18b}$$

The main processes in the CRC phase are presented in Fig. 15.

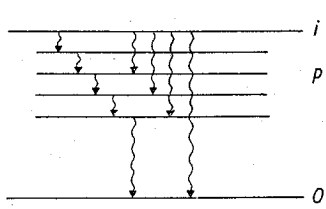

Fig. 15. The main processes in the capture radiative cascade phase (CRC) of recombining plasmas

A model for the CRC phase in astrophysical plasmas has been given by BAKER and MENZEL [33] and has been improved by SEATON [34]. From the resuls of SEATON, one can construct that

$$b(p) = \exp -(E_{ip}/kT_e) \cdot \frac{3 \ln p - \zeta(p)}{3 \ln p - \xi(p)}, \tag{19}$$

with $\zeta(p)$ and $\xi(p)$ tending asymptotically to constant values for $p \to \infty$. This implies that for very large p-values, $b(p)$ becomes 1. It means that even in this case of CRC, without any collision process or even trapping of radiation, the system tends to Saha equilibrium for very high p-values. The values of $\zeta(p)$ and $\xi(p)$ permit inversions for $\eta(p)$ or $b(p) \exp E_{ip}/kT_e$ for a large range of electron temperatures.

The dependence of population inversion on electron temperature and -density and on opacity had been investigated by FURUKANE [29] with a numerical model. He also finds inversion for rather high temperatures up till 5 eV and even higher for special circumstances. FUJIMOTO [10c, d] argues for low T_e-values a dependence according to

$$\eta(p) = p^{1,5} \tag{20a}$$

which is in line with SEATON and FURUKANE, since it also implies inversion. On the contrary, he finds for medium and high T_e-values

$$\eta(p) = p^{-0,5}, \tag{20b}$$

not in line with the findings of SEATON and FURUKANE.

4.2.2.2. Medium and High n_e-Values (ESP and PLTE)

It is clear that for increasing n_e- and p-values the CRC description breaks down since collisional processes will dominate radiative processes, according to $n_e \cdot \sum_{p+q} C(p, q) > \sum_{q<p} A(p, q)$, at first for high lying states and with increasing n_e-values, also for lower states. Radiative recombination will be taken over by three particles recombination if $n_e^2 \cdot n_i \cdot Q(p) > n_e \cdot n_i \cdot \beta(p)$. The main processes for ESP and PLTE are indicated in Fig. 16. This figure holds especially for low electron temperatures.

The collisionally dominated out of equilibrium phase for recombining plasmas is also called ESP. This phase is in the recombining case characterized by an excitation flow from higher to lower states, reversely to that in ionizing plasmas. The condition for a downward excitation flow is

$$b(p+1) > b(p) \text{ or } \delta b(p+1) > \delta b(p). \tag{21}$$

It is assumed that the description with δb is also useful for recombining plasmas with $\delta b < 0$ since these plasmas are in most cases not too far from equilibrium, so that δb is not equal to -1.

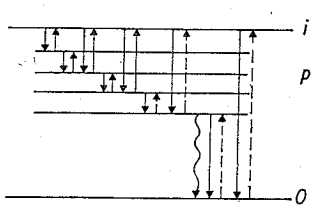

Fig. 16. The main processes in the ESP and PLTE phase of recombining plasmas with low electron temperature

It is useful to discern a high and low temperature limit, or more exactly $E_{ip}/kT_e < 1$ and $E_{ip}/kT_e > 1$. More extended theories refer to so-called bottleneck values of E_{ip}/kT_e, slightly more than 1.

For low E_{ip}/kT_e-values, in principle the same analytical treatment as given in section 6 for ionizing plasmas can be employed, since the specific ionizing character of the plasma has not been used in the derivation. It now results in

$$b(p) = 1 - b^* p^{-x}, \tag{22a}$$

thus with a minus sign instead of a plus sign (compare eq. 17), and with $x = 6$ suggested by the theory in section 6 and with $x = 5$ according to more specific theories for recombining plasmas from BIBERMAN et al [7b] and BROCKLEHURST [35]. For the great majority of p-values, the second term is of minor significance so that $b(p) \approx 1$ and $\eta(p) \approx \eta^S(p)$. It means that the ionization recombination equilibrium is so strong that the downward excitation flow causes only a minor disturbance with respect to the equilibrium value $\eta^S(p)$. The minus sign is essential for the condition that $b(p+1)$ has to be $> b(p)$ and that $\delta b < 0$. Equation (22a) allows deviations from Saha-densities, growing with decreasing p-values. According to the bottle-neck criteria, the deviations may also be limited for $p = 2$ when T_e is high enough. These predictions are roughly in agreement with data from the numerical model, described in section 5. For temperatures $T_e \geqq 2$ eV, Saha-densities are found all the way but for $T_e < 2$ eV the densities become significantly smaller than the Saha-densities, especially for low p-values.

Herewith we enter the for recombining plasmas important regime with high $u_p = E_{ip}/kT_e$-values, or low T_e-values. Now deexcitation to lower states is favoured with respect to excitation processes in upward direction. This results in a rapid fall of the distribution function of $b(p)$ for lower p-values with respect to higher ones. The most complete distribution function for this case is given by MANSBACH and KECK [36]. Their expression can be rewritten with some approximation as being

$$b(p) = \mathrm{e}^{-u_p}\,(u_p{}^3/3! + u_p{}^2/2! + u_p + 1)$$

or

$$b(p) = \exp-(Ry_0 p^{-2})\,(Ry_0{}^3 p^{-6}/3! + Ry_0{}^2 p^{-4}/2! + Ry_0 p^{-2} + 1), \tag{22b}$$

with $Ry_0 = Ry/kT_e$. For low p-values the first term dominates and for very high p-values the last term does. BIBERMAN et al [7b] find an expression with only the last constant term, but equal to about 0.6 instead of 1. FUJIMOTO [10d] only finds the p^{-6} term, valid for lower p-values. For very high p-values, the solution of $b(p)$ tends to 1, as does eq. (22a). In eq. (22b) it is expressed that $b(p)$ is for a great part dominated by the factor $\exp - Ry_0 p^{-2}$, since this factor leads to strong deviations with respect to the Saha-density for the lower p-values. The terms with p^{-6}, p^{-4} and p^{-2} are for low temperatures not sufficient to compensate fully the effect of the factor $\exp(-Ry_0 p^{-2})$. The behaviour described is confirmed by the numerical model presented in section 5 and by measurements of HINNOV and HIRSCHBERG [37], which are already used by MANSBACH and KECK to check their theory.

A phase diagram as given by FUJIMOTO [10d] for hydrogen at low temperatures is shown in Fig. 17. In Fig. 18 we indicate the $r^0(p)$ coefficients derived from DRAWIN [5b] for this case. The typical behaviour of the $r^0(p)$ coefficients is a constant value $\ll 1$ for low n_e-values in the CRC phase, a proportionality to n_e in the ESP and a constant value ≈ 1 for PLTE.

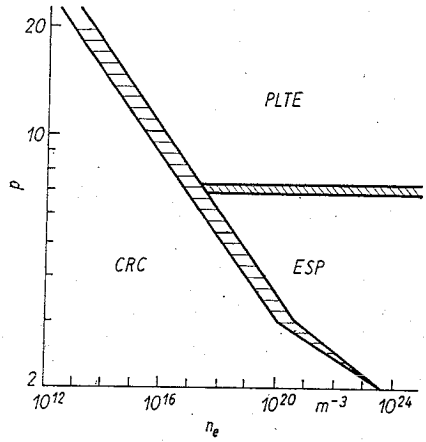

Fig. 17. A phase diagram for a low-temperature recombining hydrogen plasma at $T_e = 10^3$ K according to FUJIMOTO (10d)

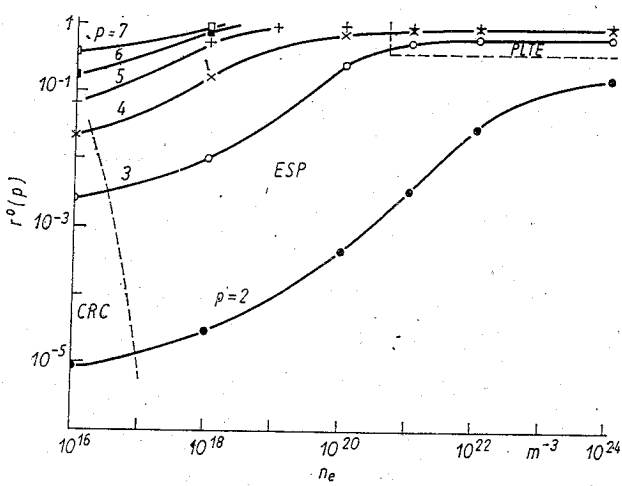

Fig. 18. The $r^0(p)$ coefficients for an optically thin, low temperature hydrogen plasma at $T_e = 4 \cdot 10^3$ K according to DRAWIN and EMARD (Ref. [5b])

4.2.3. Equilibrium Plasmas

An equilibrium plasma is a superposition of an ionizing and a recombining plasma in such a way that the eqs. (11a, b) are fulfilled. For low n_e-values there is a combination of the Corona and CRC phases. Numerical estimates of FUJIMOTO [10a] show that the densities of all excited states p are determined by Corona processes for 90% and by CRC processes for 10%. The slow radiative recombination is exceeded by a factor 10 by direct excitation from the ground state. From eq. (11) it can be deduced that the ration $n_0/n_i = \alpha_{CR}/S_{CR}$. This ratio is constant if the ionization coefficient S_{CR} and recombination coefficient α_{CR} are independent of n_e. This is the case for the Corona /CRC phase (see Fig. 19)).

For medium electron densities the ratio n_0/n_i decreases slightly, especially for optically thick plasmas. This change is mainly caused by the increase of the S_{CR} coefficient

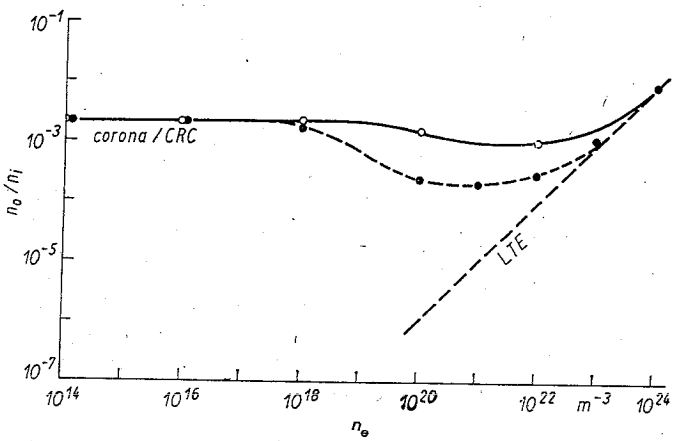

Fig. 19. The ratio n_0/n_i as a function of the electron density n_e for a hydrogen equilibrium plasma; $T_e = 32 \cdot 10^3$ K; straight line: optically thin; broken line: optically thick, $\Lambda(2,1) = 10^{-2}$, $\Lambda(3,1) = 10^{-1}$

by stepwise ionization. For medium electron densities, the net recombination coefficient α_{CR} to the ground state remains determined by radiative recombination and/or radiative decay from the lowest excited states to the ground state. Once when three particles recombination starts to dominante the recombination, we can state that for recombining processes $n(p)/n_i \sim n_e$, whereas for ionizing processes $n(p) \sim n_0$ or $n(p)/n_i \sim n_0/n_i$.

Thus this leads to a dominance of recombining processes for high n_e-values and of a linear increase of $n(p)/n_i$ with n_e. Then the LTE description is valid. It may be emphasized that the ratio n_0/n_i for ionizing plasmas may deviate orders of magnitude from that of equilibrium plasmas for low and medium n_e-values. Only for high density ionizing plasmas like cascade arcs with PLTE having minor deviations from LTE, the ratio n_0/n_i for equilibrium plasmas becomes almost equal to that of real plasmas.

5. An Example of a Numerical Model

In this section we shall describe a numerical model developed for the argon neutral system. The major question for non-hydrogenlike systems is which electron-collision cross-sections between excited states have to be used, since theoretical or measured values are in general not available. Another severe problem, specific to the numerical approach, is how many states or groups have to be taken into account to get a reliable model. Up till now, the specific results of several CR models for the argon neutral system were unsatisfactory and disagree with each other.

KATSONIS [14] describes an extended model, based on DRAWIN's excitation and ionization formulae for hydrogen. The numerical deviations of his model with respect to others are relatively large. He omitted the important $3p \rightarrow 4p$ excitation and the specific role of the 2 metastable states have not been taken into account.

VAN DER MULLEN et al [17] report on a model with only a few number of groups with an excitation between excited groups also based on DRAWIN's formulae. The ground state excitation to $4\,s$ and $4\,p$ however is taken from experimental data. They already introduce a simplified form of the excitation flow to higher states and groups.

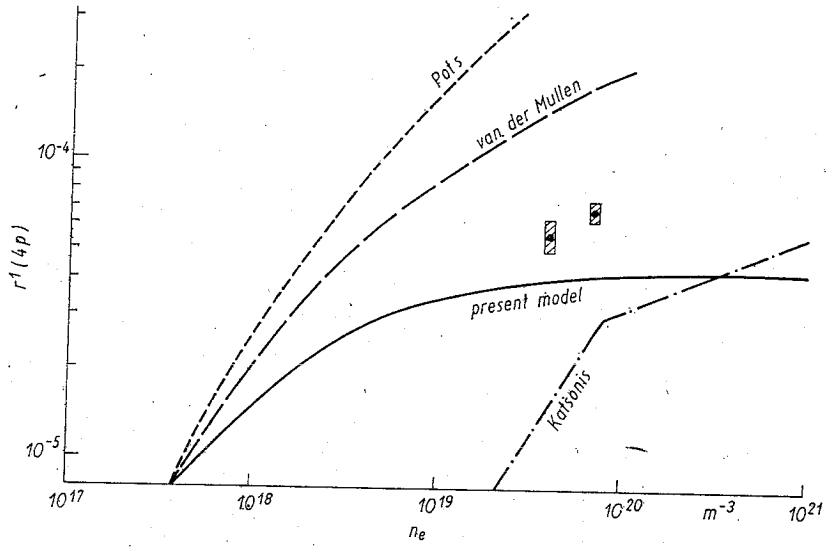

Fig. 20. The r^1 $(4p)$ coefficient for the argon neutral system for an optically thin plasma. A comparison between 4 models and measurements. For the present model the parameters are: $T_e = 3$ eV, $T_a = 1$ eV, $n_0 = 10^{19}$ m^{-3}, $R_p = 10$ mm

POTS [18] presents a model with more groups as VAN DER MULLEN, also with DRAWIN's formulae, but without introducing an excitation flow to higher states. In fig. 20 we present the $r^1(4p)$ coefficient as a function of the electron density n_e for the models discussed to illustrate the great differences with respect to each other. For all these models we see a $r^1(4p)$ course in which the typical saturation behaviour observed in experiments, namely a constant $r^1(4p)$ value, can not be found.

The main change in the model described here with respect to the previous ones is that we employ the semi-empirical excitation and ionization formulae of VRIENS and SMEETS [12] proposed for neutral hydrogen and alkali excited states. For the argon system these excitation rates appear to be a factor 5—15 larger than those of DRAWIN (see Fig. 21). These differences cause in our model the argon neutral system to be collisionally dominated for smaller n_e-values than in the previous models. The typical saturation (ESP) is shown at n_e-values, indicated by experimental data.

In the model presented here we include 49 lumped states containing groups up till the $15s$, $15p$, $14d$ and $13f$ groups. It assures a reasonably realistic excitation flow, in any case for the lower excited states and groups. The excitation cross-sections between the $3p$ ground state and the $4s$ and $4p$ groups have been deduced from experimental data [19—21]. Transition probability values have been derived from NBS-tables [22] and from KATSONIS [14].

We distinguish 4 separate $4s$ states and separate s, p, d and f groups. The s, p and d groups have been given the correct statistical weights of 12, 36 and 60 respectively. The statistical weight of the f group has been increased artificially to the value ($12p^2$—108) in order to account for the total statistical weight of $12p^2$ for each pqn p. The application of the correct total statistical weight appeared to be essential for a good result.

The trapping of resonance radiation has been taken into account. The trapping is a function of the neutral density n_0, the radius R_p, the neutral temperature T_0 (Doppler broadening) and the electron density n_e (Stark broadening).

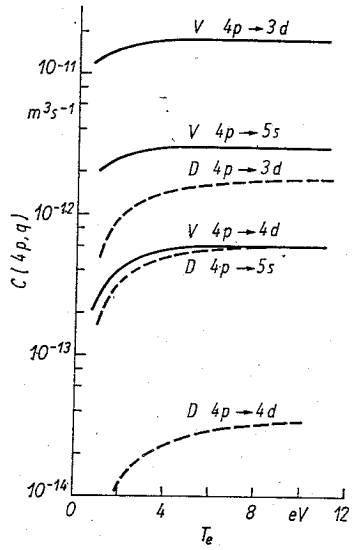

Fig. 21. A number of excitation rate coefficients as functions of T_e of VRIENS and SMEETS compared to those of DRAWIN, both applied to the argon neutral system; —— VRIENS and SMEETS; ----- DRAWIN

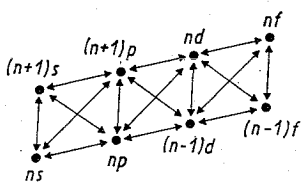

Fig. 22. The coupling scheme between the various groups in the argon neutral system

The coupling scheme for excitation between the excited states is according to:

$ns \leftrightharpoons np$; $ns \leftrightharpoons (n+1)\,s$; $ns \leftrightharpoons (n+1)\,p$;
$n(p) \leftrightharpoons (n-1)\,d$; $n(p) \leftrightharpoons (n+1)\,s$; $n(p) \leftrightharpoons (n+1)\,p$; $np \leftrightharpoons nd$;
$(n-1)\,d \leftrightharpoons (n-1)\,f$; $(n-1)\,d \leftrightharpoons (n+1)\,p$; $(n-1)\,d \leftrightharpoons nd$; $(n-1)\,d \leftrightharpoons nf$;
$(n-1)\,f \leftrightharpoons nd$; $(n-1)\,f \leftrightharpoons nf$ (see Fig. 22).

In Fig. 20 we present the $r^1(4p)$ coefficient as a function of n_e for $T_e = 3$ eV, $n_0 = 10^{19}$ m^{-3}, $T_a = 1$ eV and $R_p = 10$ mm, an optically thin plasma. In this figure the differences with the previous models and the satisfactory agreement with 2 measured values are also shown. The existence of the Corona phase ($n_e < 3 \cdot 10^{18}$ m^{-3}) and the ESP ($n_e > 10^{19}$ m^{-3}) are clearly demonstrated. This behaviour agrees with earlier measurements [23] from which it appeared that the $r^1(4p)$ coefficient did not show a significant increase for $3 \cdot 10^{19}$ m$^{-3} < n_e < 3 \cdot 10^{20}$ m^{-3}. The two indicated measured points are average values of 15—20 individual measurements of the 696.5 nm, $4p \rightarrow 4s$ line. The n_e- and T_e values have been measured with Thomson scattering and the T_e-values with Fabry-Pérot interferometry (see also ref. [38]).

In Fig. 23 we show densities of excited groups as a function of the effective pqn $p = p_{eff} = \sqrt{Ry/E_{pi}}$, for three different numbers N of groups included; R is the Rydberg

energy and E_{pi} is the ionization energy of state p. The figure clearly shows the weakness of numerical models caused by the truncation of the model at a certain group, even if a large number of groups have been included. Especially the densities of high lying groups show significant deviations caused by that fact. The slope of the straight part of the density-curve depends on the number N of considered groups. In Fig. 24 the slope of this part is indicated as a function of the number N. It shows that a sufficiently large

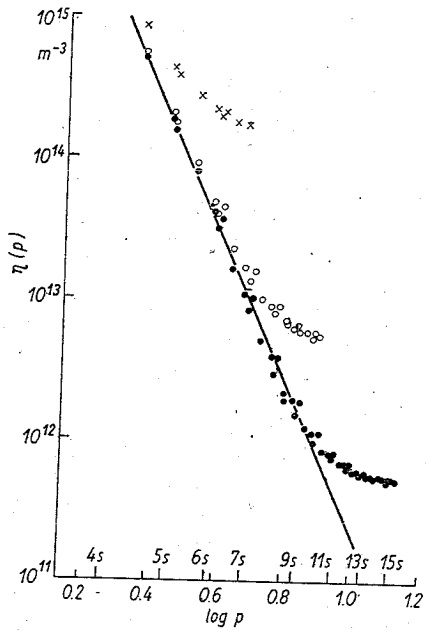

Fig. 23. The density $n(p)/g(p)$ as a function of p for three different numbers of N: 49(●), 29 (○) and 13 (×). Parameters: $n_e = 10^{20}$ m^{-3}, $T_e = 3$ eV, $n_0 = 10^{21}$ m^{-3}, $T_a = 1$ eV, $R_p = 10$ mm

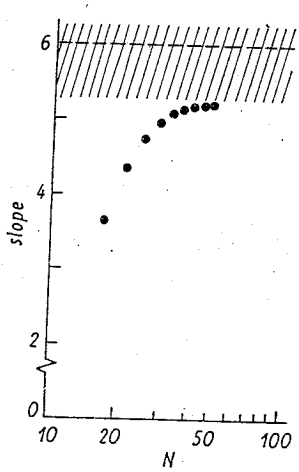

Fig. 24. The slope of the density curves as a function of N, the number of groups included

number of groups considered leads to a definite value of the slope of this straight part. It means that the density of the lower groups, roughly up to $N/2$ does not change any more. Moreover, the value of 5.2 is in satisfactory agreement with measurements and the analytical model, described in section 6. We conclude that though the truncation of the excitation flow at a certain group N to higher groups causes significant deviations in the densities of groups between $N/2$ and N, the densities of groups $< N/2$ are reliable with respect to the analytical model and experimental data if $N \geqq 40$.

In Fig. 25 we present a complete phase diagram for the parameters indicated. It is an example of an ionizing plasma.

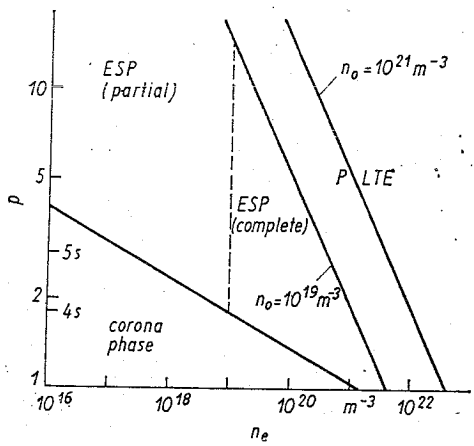

Fig. 25. The phase diagram of the argon neutral system for $T_e = 3$ eV, $T_a = 1$ eV and $R_p = 10$ mm

6. An Example of an Analytical Model

The model, developed in our group by VAN DER MULLEN et al [16], is appropriate for upper states in a real ionizing plasma. These states which are in the excitation saturation phase (ESP) or in partial local thermal equilibrium (PLTE), are described with the help of a so-called analytical top model (ATM), in principle for hydrogen and hydrogenlike ions. By application of the effective pqn p_{eff}, it can also be applied to other systems.

The main feature of an analytical model is that one general expression valid for an arbitrary state p is developed. Hence, there is no need for a truncation of the excitation flow to higher states, since this flow is contained in the general expression. Therefore, one may expect in this case a reliable slope of the density curve as a function of p. Another important point is that in the model for ESP and PLTE shown here, the numerical values of the excitation and ionization functions are of minor importance. The transition of the Corona phase to the ESP is out of the scope of this model. On the other hand, a numerical value of the excitation flow can not be deduced from the general expression for non-hydrogen systems or for parameters in hydrogen for which lower states are still in the Corona phase.

The main assumptions to be made for the analytical model presented are:

1) Radiative processes can be omitted since the plasma is collisionally dominated. It means that we only consider ESP and PLTE.

2) The excitation flow has a ladderlike character, it means that for hydrogen steps with $\Delta p = 1$ dominate over so-called jumps of $\Delta p > 1$.
3) We assume a so-called high temperature (T_e) and/or high pqn limit, so that $u_p = E_{pi}/kT_e < 1$. This assumption makes the derivation more straight-forward at some points. It is believed that this assumption plays a minor role in the results.

The balance equation of a state p then reads [16]:

$$n_e \cdot n(p-1) \cdot C(p-1, p) - n_e \cdot n(p) \cdot C(p, p-1) - n_e \cdot n(p) \cdot C(p, p+1) + n_e \cdot n(p+1) \cdot C(p+1, p) - n_e \cdot n(p) \cdot S(p) + n_e^2 n_i \cdot Q(p) = 0 \quad (23)$$

S is the ionization rate coefficient and Q the three body recombination coefficient. By defining the excitation flow $J(p)$ according to

$$J(p) = n_e \cdot n(p) \cdot C(p, p+1) - n_e \cdot n(p+1) \cdot C(p+1, p), \quad (24)$$

an ionization sink according to

$$I(p) = n_e \cdot n(p) \cdot S(p), \quad (25)$$

and a recombination source according to

$$R(p) = n_e^2 n_i \cdot Q(p), \quad (26)$$

we can state the equation

$$\mathrm{d}J(p)/\mathrm{d}p = R(p) - I(p) < 0. \quad (27)$$

This equation expresses that the change in J, $\Delta J(p) = \mathrm{d}J(p)/\mathrm{d}p \cdot \Delta p$ (with $\Delta p = 1$) is equal to the net ionization loss, $R(p) - I(p)$.
It is possible to express $C(p, p+1)$ as a simple function of p according to [16]:

$$C(p, p+1) = c_p p^4; \quad (28)$$

c_p is only a weak function of T_e and is dependent on a function ψ, which can be adjusted for the different collision theories. In the same way, $S(p)$ can be written as

$$S(p) = s_p p^2 \quad (29)$$

$Q(p)$ can be found from $S(p)$ with the principle of detailed balance. By introducing the density per statistical weight $\eta(p) = n(p)/g(p)$ and the Saha increment $b(p) = \eta(p)/\eta^S(p) = n(p)/n^S(p)$, we can deduce for $J(p)$:

$$J(p) = +\, 2 n_e \eta^S(p) \cdot c_p \cdot p^6 \{b(p) - b(p+1)\} \quad (30a)$$

which for a continuous description leads to

$$J(p) = -\, 2 n_e \eta^S(p) \cdot c_p \cdot p^6 b'(p), \quad (30b)$$

where $b'(p)$ is the first derivative of $b(p)$.
Similar expressions can be found for $I(p)$ and $R(p)$ and read:

$$I(p) = 2 n_e \eta^S(p) \cdot s_p \cdot p^4 b(p) \quad (31)$$

and

$$R(p) = 2 n_e \eta^S(p)\, s_p p^4. \quad (32)$$

By substituting the eqs. (30b, 31 and 32) into eq. (27), we can derive a second order differential equation in $b(p)$ under the assumption that $(\eta^S(p)\, c_p)' = 0$ and $(s_p/c_p)' = 0$. This is true for the high u_p limit (assumption 3). The equation reads:

$$p^2 \cdot b''(p) + 6\, p \cdot b'(p) - s_p/c_p \cdot (b(p) - 1) = 0, \tag{33}$$

with the solution:

$$b(p) = 1 + b_0 p^{-x} \tag{34a}$$

or

$$\eta(p) = \eta^S(p) + \beta p^{-x} \exp u_p \tag{34b}$$

with $b_0 = \beta \exp u_p/\eta^S(p)$.
The value of x can be found from

$$x = 2.5 + 2.5\sqrt{1 + 0.16\, s_p/c_p}. \tag{35}$$

In eq. (34) it is shown that the population distribution consists of a superposition of the Saha equilibrium value, dominant for PLTE and caused by an ionization-recombination and excitation-deexcitation equilibrium and of a term related to the excitation flow and dominant for the ESP. This term can be considered as an overpopulation $\delta b = b_0 p^{-x}$ with respect to the Saha density.

It can be concluded from eq. (35) that variation of the value s_p/c_p, e.g. from different collision theories has only a minor influence on the value of x; x is always > 5 and close to 6. In Ref. [16] it is pointed out that for $x = 6$ the solution $\beta p^{-x} \exp u_p$ has the same energy dependence as the Maxwell distribution for free electrons. This surprising result can be understood by noting that in the ESP the interactions with free electrons occur more frequently than typical atomic events like radiative decay. Apparently, the result of these frequent interactions is that the energy distribution of the free electrons is imposed on the overpopulated bound electrons. It is also shown that the derivation of the distribution function can be carried out with a Fokker-Planck description without assuming the $\Delta p = 1$ limitation for excitation.
With the solution for $\eta(p)$ with $x = 6$ we can find

$$J(p) = 12 n_e \beta c_p p^{-1} \exp u_p, \tag{36a}$$

$$I(p) = 2 n_e \beta s_p p^{-2} \exp u_p + 2 n_e \eta^S(p)\, s_p p^4 \tag{36b}$$

and

$$R(p) = 2 n_e \eta^S(p)\, s_p p^4. \tag{36c}$$

In Fig. 26 the results for $J(p)$, $I(p)$ and $R(p)$ as functions of p are shown for different n_e-values. $J(p)/n_e$ is monotonously decreasing as a consequence of the fact that $R(p) - I(p) < 0$ for every p-value. Also $I(p)/n_e$ is a monotonously decreasing function with p^{-2}, as far as the first term is considered. This term can be explained as the net ionization, the difference between $I(p)$ and $R(p)$. $R(p)$ itself, and hence $I(p)$ increase rapidly with p and with n_e and from a certain p-value p^* the term $2 n_e \eta^S(p)\, s_p p^4$ becomes dominant. If the second term of $I(p)$ or $R(p)$ becomes larger than the first term, we are leaving the ESP and entering PLTE. The basic importance of Fig. 26 is that the ESP solution represented by $J(p)$ and the first term of $I(p)$ is valid for all p-values and dominates for $p < p^*$ and that the PLTE solution represented by the second term of $I(p)$ and by $R(p)$ is also valid for all p-values but dominates for $p > p^*$.

In Fig. 27 we show that there is very good agreement between expression $\chi(p) = \eta(p) \exp\text{-}u_p \sim p^{-6}$ and a number of experiments in different gases, as e.g. Na I, He II and Ar I. It means that the collisionally dominated top of a spectral system can be satisfactorily described with a simple power law.

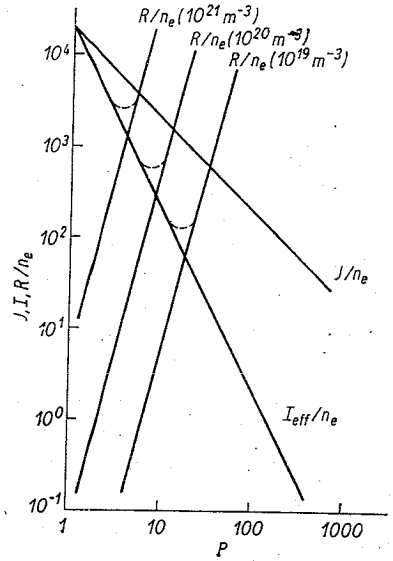

Fig. 26. The excitation flow $J(p)/n_e$, the ionization sink $I(p)/n_e$ and the recombination source $R(p)/n_e$ as functions of p for different n_e-values; $T_e = 4$ eV, $n_e = 10^{19}$ m^{-3}, (for $J(p)$, $I(p)$, $n_0 = 10^{19}$ m^{-3}

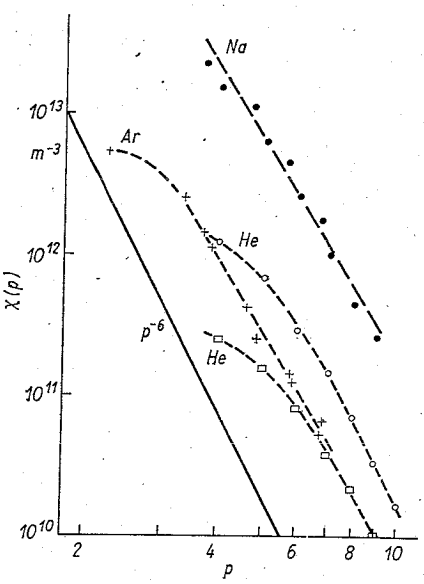

Fig. 27. Comparison between the analytical expression $\chi(p) \sim p^{-6}$ and a number of experiments:

+ argon I Ref. [24]

□○ helium Ref. [25]

• sodium Ref. [26]

7. Conclusions

1. Especially the work of SEATON, FUJIMOTO, BIBERMAN et al, and DRAWIN et al make it possible nowadays to have at our disposal a systematic, and in many cases quantitative description of collisional radiative models of spectroscopic systems in plasmas.
2. The global character of the description of analytical models as e.g. from FUJIMOTO has been extended to more fundamental descriptions by SEATON and BIBERMAN et al and especially for the ESP and PLTE of ionizing plasmas by VAN DER MULLEN et al. By these contributions, a simple but reliable description for the upper part of excited systems is available.
3. It appears to be possible to extend the set-up of numerical models from hydrogen (like) systems to more complex systems as e.g. the argon neutral system with the help of the formulae of VRIENS and SMEETS with a satisfactory agreement with experimental data. The p^{-6} dependence, found in the analytical model for the ESP, appears to be produced by the numerical model with reasonable accuracy.
4. The comparison between analytical and numerical models delivers more insight into the possibilities and limitations of both models. Examples of these are:
   1) The limitation of a numerical model due to the cut-off at a certain state. A sufficient number of states has to be taken into account and only for the half of this number reliable results are found. At the other hand, one can extrapolate the results for the lower states with sufficient accuracy to the higher states. The experience of the analytical model is a helpful guide in this.
   2) The limitation of an analytical model to a specific phase deserves another analytical model or a limited numerical model to make possible an absolute rather than a relative computation of state densities, at the other hand. The analytical model provides one generally valid solution for a great number of states without a time-consuming set-up of an extended numerical model.
   3) The analytical model for the collisionally dominated phases ESP and PLTE is less sensitive to the specific collision theory used, whereas numerical models, including the corona phase and ESP are very sensitive to this choice.
   4) Integration of analytical and numerical models promises the best results with a minimum of work, so that the advantages of both are realized.

References

[1] BATES, D. R., KINGSTON, A. E., and MCWHIRTER, R. W. P., Proc. Roy. Soc. **A 267** (1962) 297; **A 270** (1962) 155.
[2] MCWHIRTER, R. W. P., and HEARN, A. G., Proc. Phys. Soc. **82** (1963) 641.
[3] GRIEM, H. R., Phys. Rev. **131** (1963) 1170.
[4] DRAWIN, H. W., Ann. der Physik **14** (1964) 262, Zeitschr. f. Physik **186** (1965) 99.
[5] CACCIATORE, M., CAPITELLI, M., and DRAWIN, H. W., Physica **84 C** (1976) 267; DRAWIN, H. W., and EMARD, F., Physica **85 C** (1977) 333 and **94 C** (1978) 134; DRAWIN, H. W., Physica **103 C** (1981) 448.
[6] BIBERMAN, L. M., VOROB'EV, V. S., and YAKUBOV, I. T., High Temperature **5** (1967) 177; **6** (1968) 359; **7** (1969) 183; **7** (1969) 543 (original Teplofizika Vysokikh Temperatur **5** (1967) 201; **6** (1968) 369; **7** (1969) 193; **7** (1969) 593).
[7] BIBERMAN, L. M., VOROB'EV, V. S., and YAKABOV, I. T., Sov. Phys. Uspekhi **15** (1973) 375 and **22** (1979) 411 (original Uspekhi Fizicheskikh Nauk **107** (1972) 353 and **128** (1979) 233).
[8] FUJIMOTO, T., OGATA, Y., SUGIYAMA, I., TACHIBANA, K., and FUKUDA, K., Jap. J. Appl. Phys. **11** (1972) 718; TACHIBANA, K., and FUKUDA, K., Jap. J. Appl. Phys. **12** (1973) 895.
[9] FUJIMOTO, T., J. Phys. Soc. Japan **34** (1973) 216.

[10] FUJIMOTO, T., J. Phys. Soc. Japan **47** (1979) 265; **47** (1979) 273; **49** (1980) 1561; **49** (1980) 1569.
[11] JOHNSON, L. C., Astrophys. J. **174** (1972) 227.
[12] VRIENS, L., and SMEETS, A. M. M., Phys. Rev. **A 22** (1980) 940.
[13] FUJIMOTO, T., JOSRT **21** (1978) 439.
[14] KATSONIS, K., thesis Université Paris Sud, 1976.
[15] POTS, B. F. M., VAN DER SIJDE, B., and SCHRAM, D. C., Physica **94 C** (1978) 369.
[16] VAN DER MULLEN, J. J. A. M., VAN DER SIJDE, B., and SCHRAM, D. C., Proc. 15th ICPIG, Minsk, USSR 1981, p 441; Phys. Letters **96 A** (1983) 239.
[17] VAN DER MULLEN, J. J. A. M., VAN DER SIJDE, B., POTS, B. F. M., and SCHRAM, D. C., Proc. 13th ICPIG, Berlin, DDR 1977, p 323.
[18] POTS, B. F. M., Thesis University of Eindhoven, 1979.
[19] LLOYD, C. R., WEIGOLD, E., TEUBER, P. J. O., and HOOD, S. T., J. Phys. B **5** (1972) 1712.
[20] CONKEY, J. W. Mc., and DONALDSON, F. G., Can. J. Phys. **51** (1973) 914.
[21] PETERSON, L. R., and ALLEN, I. E., J. Chem. Phys. **56** (1972) 6068.
[22] WIESE, W. L., SMITH, M. W., and MILES, B. M., Atomic Transition Probabilities, Part II, Nat. Bur. Stand. (1969).
[23] VAN DER SIJDE, B., VAN DER MULLEN, J. J. A. M., POTS, B. F. M., SCHRAM, D. C., D. P. G. Tagung, Hamburg (BRD) 1981, p. 894;
VAN DER SIJDE, B., POTS, B. F. M., SCHRAM, D. C., VAN DER MULLEN, J. J. A. M., Proc. 5th ESCAMPIG, Dubrovnik, Yugoslavia, 1980, p. 123.
[24] VAN DER MULLEN, J. J. A. M., VAN DER SIJDE, B., SCHRAM, D. C., Physics Letters **79 A**, (1980) 51.
[25] KOHSIEK, W., JQSRT **16** (1976) 1079.
[26] VRIENS, L., J. Appl. Phys. **49** (1978) 3814.
[27] VAN DE REE, J., Phys. Rev. A **25** (1982) 1181.
[28] JACOBS, V. L., DAVIS, J., and ROGERSON, J. E., JQSRT **19** (1978) 591;
DAVIS, J., and JACOBS, V. L., JQSRT **24** (1980) 283.
[29] FURUKANE, U., YOKOTA, T., and ODA, T., JQSRT **22** (1979) 239;
FURUKANE, U., TSUJI, Y., and ODA, T., JQSRT **27** (1982) 557;
FURUKANE, U., YOKOTA, T., KAWASAKI, K., and ODA, T., JQSRT **29** (1983) 75.
[30] DIELIS, J. W. H., DE HOOG, F. J., and SCHRAM, D. C., J. Appl. Phys. **51** (1980) 5708.
[31] VAN ODENHOVEN, F. J. F., thesis Eindhoven University of Technology (1983).
[32] VAN VELDHUIZEN, E. M., thesis Eindhoven University of Technology (1983).
[33] BAKER, J. G., and MENZEL, D. H., Astroph. J. **88** (1938) 52.
[34] SEATON, M. J., Mon. Not. Roy. Astr. Soc. **119** (1959) 90.
[35] BRUCKLEHURST, M., Mon. Not. Roy. Astr. Soc. **148** (1970) 417.
[36] MANSBACH, P., and KECK, J., Phys. Rev. **181** (1969) 275.
[37] HINNOV, E., and HIRSCHBERG, J. G., Phys. Rev. **125** (1962) 795.
[38] VAN DER SIJDE, B., ABU-ZEID, O., WIJSHOFF, H. M. A., Phys. Letters **101 A** (1984) 491.

Received July 12, 1983; revised manuscript received November 28, 1983